THE EXTRACTION LAMBERTSON SEPTUM MAGNET OF THE SNS *

J. Rank, G. Miglionico, D. Raparia, N. Tsoupas, J. Tuozzolo, Y.Y. Lee
Collider-Accelerator Department, Brookhaven National Laboratory, Upton, NY 11973, USA

Abstract

In the Spallation Neutron Source, after multiple injections to an accumulator ring, a final extraction delivers the full proton beam to the target, achieved by a series of kickers and a thin septum magnet. Here we discuss the lattice geometry, beam dynamics and optics, and the vacuum, electromagnetic and mechanical design aspects of the Extraction Lambertson Septum Magnet (ELS). Relevant datum are established. Vector calculus is solved for pitch and roll angles, which are shown schematically in magnet sections.

INTRODUCTION

The ELS magnet intercepts then redirects the proton beam on extraction cycles, yet passes undisturbed the ring's circulating beam on accumulation cycles. The Extraction Region (ER) straight section of the accumulator ring (Fig. 1) consists of, consecutively: A set of pulsed Kickers [1] which bump the beam at a downward "kick angle" in the vertical plane; the subject Lambertson Septum magnet; and finally the Quadrupole Doublets that focus and correct beam projection to target.

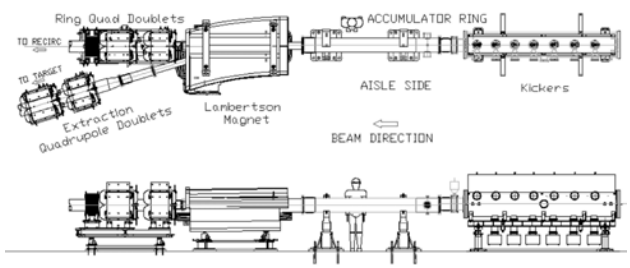

Figure 1: SNS Extraction Region plan and elevation views.

DESIGN CRITERIA

ELS design satisfies the constraints of the ER lattice specification: That the intercepted beam entering at the kicked angle ($\alpha_{EB\,CL}$) finally exits to the transfer line on a path lying in a horizontal plane at the established target elevation (Fig. 2), and at an exit angle (θ) relative to the ring as dictated by the lattice to-target projection (Fig. 3). Specifically for SNS, with predetermined target elevation, at the first quadrupole beam center is displaced vertically from magnet center. This introduces a small dipole component that corrects for a slight angular offset from the horizontal (β).

To avoid compound error in 400 circulation passes per extraction cycle, we optimize electromagnetics for the circulating beam in the ring (CB). To this end, at beam entrance and exit the yoke design features iron squared to the CB path rather than the extracted beam (EB) path, in order to minimize quadrupole affects on the CB.

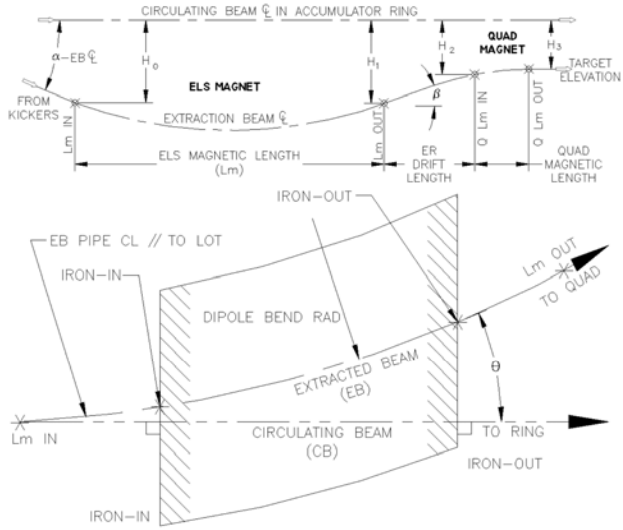

Figures 2 & 3: ER elevation (above) & plan view schematics.

Provision is also made to capture the CB within a shield assembly consisting of the "septum plate" and the "shield plate" (Fig.4). "Clamshelled" between these plates the CB vacuum chamber is wrapped in a thin non-magnetic shimstock to provide an effective impedance to flux to which the CB would otherwise be exposed. A narrow "shield cap" runs along the CB axis flush with the shield assembly. The total iron thickness (minus CB pipe) yields a flux density within iron saturation limits, both at the entrance in the thin septum, and near the exit despite return path asymmetry from the CB outboard of the ELS centerline. Along the beam direction the iron overhang shields the "sandwiched" CB beyond the ELS fringe field.

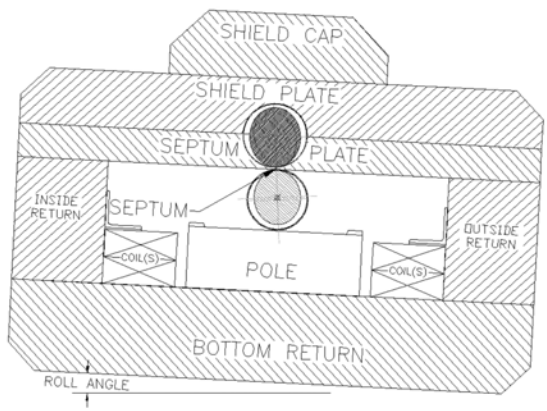

Figure 4: World x-y plane section at beam entrance to yoke.

OPTICS AND GEOMETRY

Of four SNS operating modes, ELS design is based on physics parameters for the largest beams. In all modes the elliptical beam sections of both CB and EB diverge along both major and minor axes (y and x, respectively). The y-axis divergence of the EB, and the known kick angle of the EB centerline, ultimately determine ELS magnetic geometry. To maximize septum thickness each vacuum pipe remains always tangent to the major axes of the beam it contains; i.e., CB and EB points-of-tangency (POT) occur at 6 and 12 o'clock orientations respectively (Fig. 5). Thus pole (magnet yoke) geometry must be everywhere parallel to the EB pipe centerline. This pipes diameter is determined by the EB size at the exit, and thus fixes the magnetic gap; the distance between the primary pole and the septum quasi-pole (Fig. 6). Similarly, there exists an angular offset of the CB with respect to its vacuum pipe which determines the axis of the cut hole in the shield assembly. These angular offsets are corrected at both exit flanges with "skewed" bores which center the beam path in the downstream pipe. Bore angles are offset also at the upstream "crotched" entrance flange. The shim "air gap" runs the length of the magnet including shielding porches, but terminates at the "field clamp". The clamp, in contact with the magnetic CB pipe, closes the electromagnetic circuit at end of air gap for

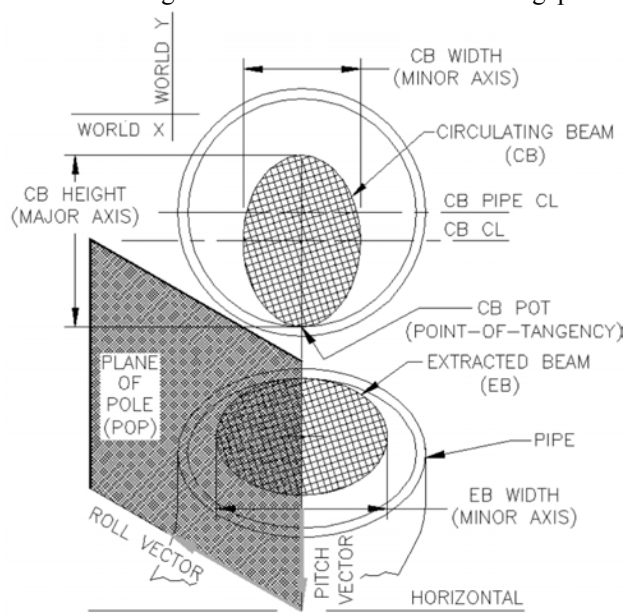

Figure 5: Schematic of world x-y section at beam entrance.

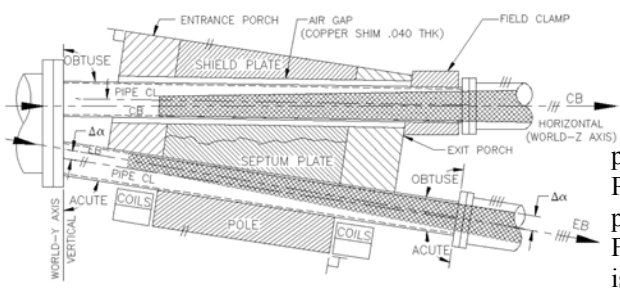

Figure 6: Schematic of world x-z section through pipe centers.

Recalling ELS design criteria, entering beam kicked downward relative to a world horizontal plane (WCS x-z) exits in that plane at a lattice-prescribed height and angle. Thus yoke geometry cannot be orthogonal to *any* WCS axis; i.e., the plane-of-pole (POP) first must lie tangent to an axis pitched about the world-x in order to receive the entering kicked beam, and second must be rolled about that pitch-axis in order to project the exiting beam at the given extracted angle, but parallel to the WCS x-z plane (or nearly; section 2). To gain pipe-to-diverging-beam tangency, pipe rotation about the world-x is by the kick angle ($\alpha_{EB\ CL}$) less the EB y-radii divergence angle ($\Delta\alpha$).

$$\overline{V_{pop}} := \left(\overline{V_{wcs}}\cdot[T_{pitch}]\right)\cdot[T_{roll}] \text{ where } \overline{V_{pop}} := \left(V''_x \;\; V''_y \;\; V''_z\right) \text{ thus}$$

$$\frac{V''_x}{V_{wcs}} := \left[\sin(\gamma)\cdot\left[\frac{\tan(\theta)}{\tan(\gamma)} + \sin(\alpha)\cdot\left(1 - \frac{\tan(\beta)}{\tan(\alpha)\cdot\cos(\theta)}\right)\right]\right]$$

$$\frac{V''_y}{V_{wcs}} := \left[\cos(\gamma)\cdot\left[\tan(\gamma)\cdot\tan(\theta) - \sin(\alpha)\cdot\left(1 - \frac{\tan(\beta)}{\tan(\alpha)\cdot\cos(\theta)}\right)\right]\right]$$

$$\frac{V''_z}{V_{wcs}} := \left[\cos(\alpha)\cdot\left(1 + \frac{\tan(\alpha)\cdot\tan(\beta)}{\cos(\theta)}\right)\right] \text{ where } \begin{matrix}\alpha \text{ is pitch angle}\\ \gamma \text{ is roll angle}\end{matrix}$$

$$\text{Given } \left(V''_x\right)^2 + \left(V''_z\right)^2 := V_{wcs} \text{ and } V''_y := 0 \text{ solve for } \alpha, \gamma$$

Figure 7: POP to WCS coordinate transformation.

To relate ELS pole coordinate system (POP CS) to the customary perspective for a conventional dipole in the WCS, one must perform a series of two coordinate transformations. Mathematically, the matrix algebra of Fig. 7 is solved for both the divergence-corrected pitch angle (α_{LOT}) and the roll angle (γ) given constraints on lattice geometry (β & θ of Fig. 2 & 3). Visually, we first rotate the viewing direction in Fig. 5 by the corrected pitch angle (Fig. 8), then by the roll angle (Fig. 9).

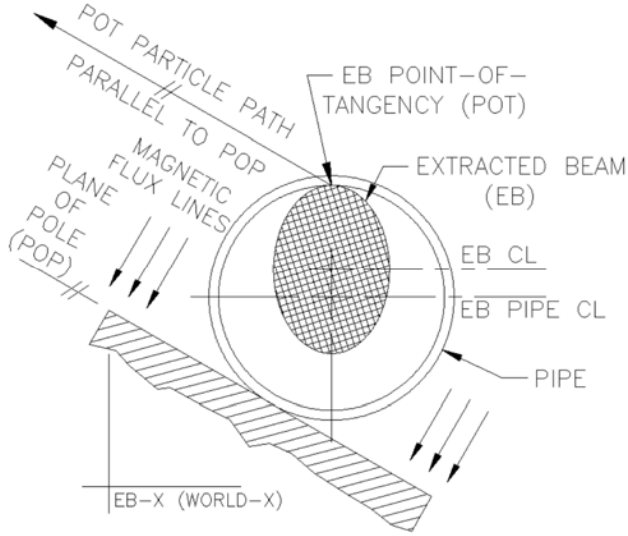

Figure 8: Pitch-corrected view of EB and pole.

We may resolve the velocity vector ***v*** of an arbitrary particle entering ELS field into components orthogonal to POP; i.e., aligned with the flux lines (POP-y axis, perpendicular to the pole), or lying in the POP (POP x-z). Fig. 10 depicts a particle on the LOT path. The vector ***v*** is resolved into components orthogonal to the POP CS. The resultant of vectors parallel to the POP is ***v // POP***.

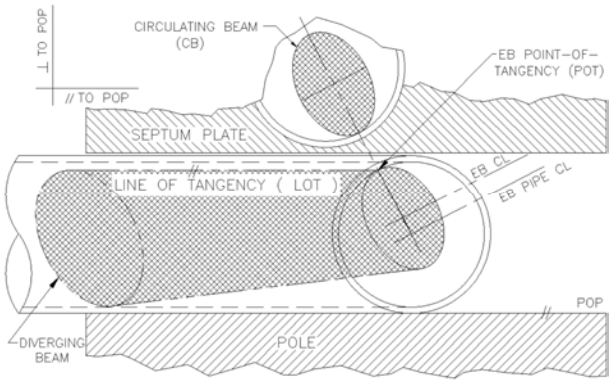

Figure 9: POP x-y plane section schematic at beam entrance.

Bend radius due to ELS field is proportional to ***v // POP*** ; but the component perpendicular to POP remains constant along the particle path. Thus only a particle positioned at the EB POT will travel on a circular arc always parallel to the POP; this line-of-tangency (LOT) arc shows in Fig. 9. All others, including those on beam center, have constant non-zero POP-y velocity component. Hence, the EB path through the ELS is a helix; the particle bunch appears as a "horn on a table" in contact on its LOT. This adds subtle complexities to 3D model development, lattice placement, and specification of survey and alignment at installation. A datum point used to place a conventional dipole, where entering and exiting centerlines intersect, does not exist.

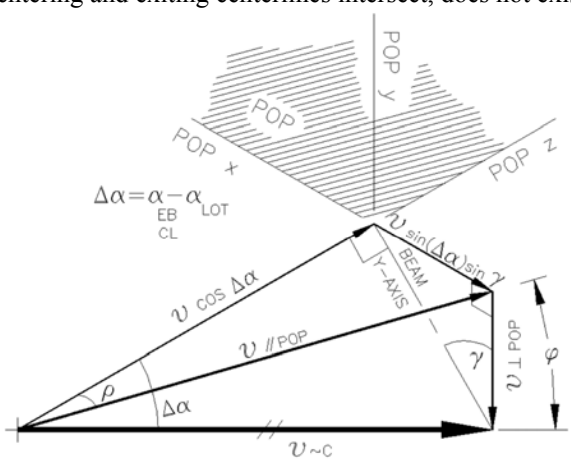

Figure 10: Velocity vector POP components for LOT particle.

Figure 11: ELS magnet assembly looking upstream.

ELS MAGNET ASSEMBLY

A discussion of design issues for the various components of the ELS magnet assembly (Fig. 11 and 12) is useful.

Coils

Water-cooled coils, sized for 1.3 GeV, have the following specifications: Allowable 20^0C rise, 70 psid max, 5-15 fps turbulent flow, and current density <1000 A/sq. cm. [2]. A centertap divides the very long cooling circuit of the continuous conductor. Radiation exposure of septa generally warrant consideration of "rad-hard" coils.

Vacuum Chamber

Chamber manufacture requires many stages. The CB pipe from ASTM A513 DOM tube for dimensional accuracy, is placed in an acid bath, vacuum fired, masked at the weld joints, and nickel plated inside and out. The tube is welded to 304L flanges of the now-formed EB weldment, including the delicate weld at the crotch. Care is taken here as the weld is compounded by: a thin base metal, a tight fit, dissimilar metals, a fragile nickel plating, and high stresses. Finally, the tube is TiN coated.

Shielding and Yoke

Kicker design limits septum thickness; as weighed against competing concerns of saturation and stress. A half-circular cut in both septum and shield plates provide a close fit clamshell to insure accurate location of the CB tube. Allowable stack-up tolerance for this machining process, and for plate flatness and vacuum pipe geometrical tolerances, depends on beam emittance. Pole design is based on field uniformity requirement. The ELS pole has no square faces (Fig. 3). Porches from steel laminations shield the CB from local fringe field, and intercept any stray field away from the CB. A field clamp bolts to CB tube and to the porches; this reacts vacuum load on the chamber from the upstream ER bellows.

Figure 12: ELS magnet assembly looking downstream.

REFERENCES

[1] C. Pai, et. al., "Construction and Power Test of the Extraction Kicker Magnet For Spallation Neutron Source Accumulator Ring", these proceedings.

[2] Jack Tanabe, SLAC, Accelerator Magnet Engineering, USPAS 2001

